

We have investigated the use of the $\alpha,\alpha,\alpha,\alpha$ -isomers of aryl-extended calix[4]pyrroles in the complexation of polar guests in aqueous solution through a combination of hydrogen-bonding, CH- π , π - π , and hydrophobic interactions.^[16,17] In the cone conformation, the tetra- α -isomers feature a deep aromatic cavity that is open at one end and closed at the opposite one by four pyrrole NH moieties. We also reported the installation of bridging polar phosphonate groups at the upper rim of phenoxy tetra- α -calix[4]pyrroles.^[18,19] Simple molecular-modelling studies predicted that the neutral creatinine tautomer **2** would be a perfect fit in terms of size and hydrogen-bonding complementarity to the polar aromatic cavity offered by monophosphonate-bridged cavitand **1**. Receptor **1** was prepared starting from a previously reported aryl-extended tetrol calix[4]pyrrole.^[20,21]

The ^1H NMR spectrum of **1** in CD_2Cl_2 solution showed sharp and well-resolved proton signals that were in agreement with its C_s symmetry (Figure 2b,d). Taking into account the well-known low solubility of neutral creatinine (**2**) in organic solvents,^[9] we performed solid-liquid extraction experiments. An excess of solid neutral creatinine **2** was added to a 1 mM CD_2Cl_2 solution of **1**. The resulting suspension was hand-shaken for several minutes and filtered. The filtered solution

was analyzed by ^1H and ^{31}P NMR spectroscopy. The ^1H NMR spectrum showed a single set of proton signals for **1** with significant changes in chemical shift compared to those observed in the absence of the guest (Figure 2a,c).

From the perspective of understanding the binding process and the geometry of the complex, the most relevant shift changes occurred to the three signals belonging to the NH pyrrole protons (with an integral ratio of 1:1:2). These signals moved downfield ($\Delta\delta \approx 1.7$ –2.0 ppm), suggesting their involvement in hydrogen-bonding interactions with the bound creatinine guest. Two new singlets corresponding to the methyl and methylene protons of extracted creatinine **2** appeared at $\delta = 2.59$ ppm (CH_3) and 1.06 ppm (CH_2 ; Figure 2c). When compared to the chemical shifts of neutral creatinine (**2**) in $[\text{D}_6]\text{DMSO}$ solution, these protons resonate significantly further upfield ($\delta = 2.9$ ppm for CH_3 , $\Delta\delta \approx -0.36$ ppm; $\delta = 3.6$ ppm for CH_2 , $\Delta\delta \approx -2.54$ ppm). The large upfield shifts experienced by the methylene protons of bound creatinine (**2**) strongly suggested its deep inclusion in the aromatic cavity of **1**. The relative intensities of the resonances corresponding to **1** and **2** indicated that one equivalent of creatinine had been extracted. 2D NOESY and ROESY experiments further confirmed the proposed binding geometry (see the Supporting Information, Figures S2–S5). Taken together, these results show that neutral creatinine (**2**) forms a thermodynamically highly stable inclusion complex with receptor **1**. The oxygen atom of neutral creatinine (**2**) established four convergent hydrogen bonds with the pyrrole NH groups; one additional hydrogen bond was formed between the NH group of creatinine and the oxygen atom of the P=O group. The creatinine methylene hydrogen atoms were involved in CH- π interactions with two of the aromatic substituents at the meso positions. The significant coverage of the creatinine surface offered by inclusion complex **2**:**1** represents a breakthrough with respect to previous receptors for this analyte. Assuming that the solubility of neutral creatinine (**2**) in CD_2Cl_2 is lower than 1×10^{-5} M and the exclusive formation of a 1:1 inclusion complex, we estimated the lower limit of the stability constant $K(\text{2}:\text{1})$ to be $1 \times 10^7 \text{ M}^{-1}$ (complex/free host ratio > 100). Slow evaporation of a dichloromethane (DCM) solution yielded single crystals of the **2**:**1** complex that were suitable for X-ray diffraction. Figure 3a shows the structure of the inclusion complex **2**:**1** in the solid state.^[22] This structure is in good agreement with the solution NMR studies and molecular modelling studies in the gas phase.

With the aim to understand the role of the phosphonate group in **1**, we performed extraction experiments with creatinine (**2**) and doubly methylene-bridged receptor **3**, which is identical to cavitand **1**, but lacks the phosphonate group (Figure 1). In acetone solution, receptor **1** extracted 0.40 equivalents of **2** (Figure S6), whereas the creatinine proton signals were not detected in control extraction experiments with reference receptor **3** or in the absence of any receptor. This result clearly supported the importance of hydrogen bonding between the guest NH moieties and the inwards-pointing PO group for increasing the binding affinity of **1** towards creatinine **2**.

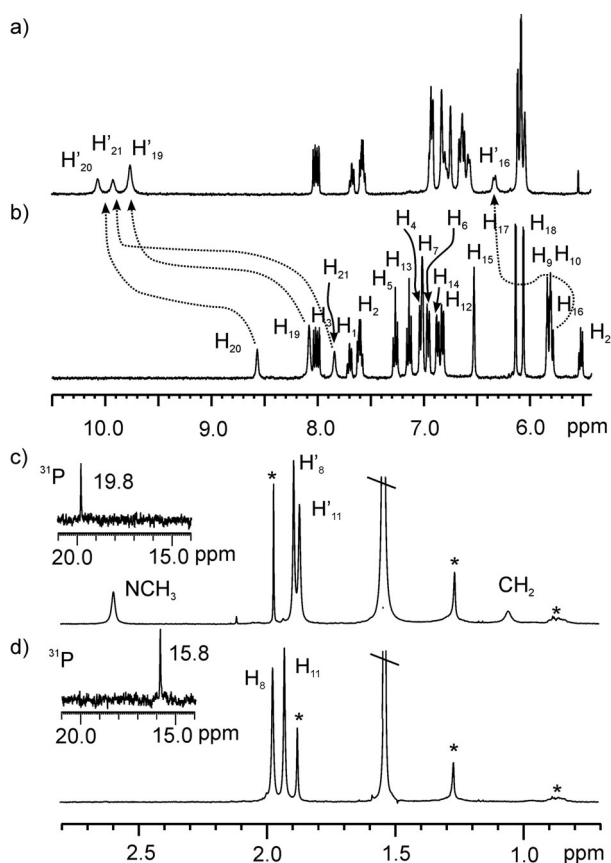


Figure 2. Selected downfield (a,b) and upfield (c,d) portions of the ^1H NMR spectra of monophosphonate cavitand **1** in CD_2Cl_2 (b,d) and the corresponding filtered solution obtained after a solid-liquid extraction experiment with creatinine (a,c). The corresponding ^{31}P NMR spectra are shown as insets in (c) and (d). * refers to impurities.

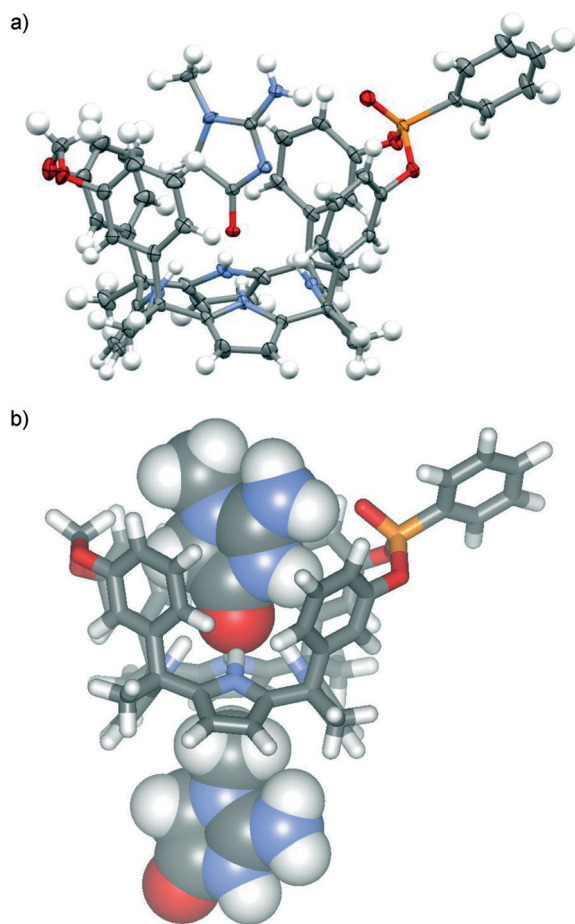


Figure 3. a) Side view of the X-ray structure of the inclusion complex 2C1. Thermal ellipsoids set at 50% probability; the H atoms are shown as spheres of 0.3 Å. b) Energy-minimized structure of the putative 2:1 complex (2·H⁺)₂C1.

In theory, to function as an ionophore in a creatinine ISE, the receptor must bind the protonated form of creatinine, 2·H⁺, which leads to charge separation across the membrane interface, culminating in a voltage reading. For this reason, we evaluated the interaction of the creatininium cation (2·H⁺) with receptor **1** and bis(methylene)-bridged receptor **3** as a reference compound.

Owing to the known binding affinities of calix[4]pyrroles for anions and ion pairs,^[23] we selected tetrakis(3,5-bis(trifluoromethyl)phenyl)borate (BARF; Figure 1) as a solubilizing and non-competitive counterion for the creatininium cation. The prepared salt, BARF[−]·2·H⁺, was readily soluble in DCM. We performed NMR titration experiments with receptors **1** and **3** by adding incremental amounts of BARF[−]·2·H⁺ (Figure S7). The pyrrole NH protons of both receptors experienced downfield shifts. However, the extent of the shift was reduced, especially for **3**, when compared to the $\Delta\delta \approx 2$ ppm shift observed for **1** upon formation of the 2C1 complex. Based on literature precedents,^[24] and our own X-ray structure of BARF[−]·2·H⁺ (Figure S17), protonation of creatinine occurs at the nitrogen atom of the five-membered heterocycle (Figure 1). Protonation at this position is likely to substantially reduce the hydrogen-bonding-accepting proper-

ties of the adjacent carbonyl oxygen atom and might account for the reduced downfield shift of the NH protons of the receptor upon binding of 2·H⁺. Interestingly, during the ¹H NMR titration experiment with **1** and BARF[−]·2·H⁺, we observed that the β -protons of the pyrrole rings not included in the 14-membered macrocycles (H₉ and H₁₀, Figure 1) experienced a non-monotonic change in chemical shift (Figure S7). This titration behavior is typically observed when complexes with a stoichiometry that deviates from a simple 1:1 ratio are formed. Indeed, a good fit of the titration data for H₉ and H₁₀ was achieved with a theoretical binding model that assumed the formation of two complexes with 1:1 and 2:1 (2·H⁺/receptor) stoichiometries. From the fit, we calculated the binding constants for the two complexes to be $K((2\cdot H^+)\cdot 1) = 1.6 \times 10^4 \text{ M}^{-1}$ and $K((2\cdot H^+)_2\cdot 1) = 0.8 \times 10^3 \text{ M}^{-1}$. We propose that in the 1:1 complex, the 2·H⁺ cation is preferentially included in the deep and polar aromatic cavity of **1**, resulting in a binding geometry that is similar to the one observed for the inclusion complex of neutral creatinine in the 2C1 complex. The interaction of the 2·H⁺ cation with the PO group of **1** was also supported by chemical shift changes observed in the ³¹P NMR spectra acquired throughout the titration experiment. Upon increasing the concentration of 2·H⁺, the initially formed 1:1 complex bound an additional 2·H⁺ cation in the shallow and electron-rich cavity defined by the pyrrole rings to produce a 2:1 complex. In short, the creatininium cation, 2·H⁺, showed a reduced binding affinity towards receptor **1** compared to its neutral counterpart and a dual binding mode.

The titration of the reference receptor, bis(methylene)-bridged derivative **3**, with BARF[−]·2·H⁺ was indicative of the exclusive formation of a 1:1 complex ($K((2\cdot H^+)\cdot 3) = 1.0 \times 10^3 \text{ M}^{-1}$). The complexation induced chemical-shift changes for the methyl and methylene protons of the 2·H⁺ cation suggested that the creatininium cation was not included in the deep and polar aromatic cavity of **3**. Instead, the 2·H⁺ cation was located in the shallower and electron-rich cavity defined by the pyrrole rings. A 2D ROESY experiment also supported the hypothesis that the cation is located in this cavity (“exo”) (Figure S16). Clearly, the lack of the upper-rim PO group was responsible for the selective inclusion of 2·H⁺ in the shallow cavity of **3** and the exclusive formation of an exo 1:1 complex, 2·H⁺·**3**, with reduced thermodynamic stability compared to the endo 2·H⁺·**1** complex.

The working principle of the ISE is based on the partition equilibrium of 2·H⁺ at the membrane phase boundary (Figure S18). This is the origin of the electrical potential that ideally solely depends on the activity of the creatinine ions ($a_{\text{creatinine}}$). To demonstrate the superior properties of ionophore **1**, we built (see the Supporting Information) and tested three distinct electrodes with identical polymeric membrane compositions. We used PVC as the polymer component, *ortho*-nitrophenyl octyl ether (*o*-NPOE) as the plasticizer, and potassium tetrakis[3,5-bis(trifluoromethyl)phenyl]borate (KBARF) as the ion exchanger. All of the membranes were prepared with 30 mol% of the ion exchanger with respect to the ionophore and with polymer and plasticizer in a weight ratio of 1:2. Whereas the “blank” sensor does not contain any embedded ionophores, sensors **1** and **2** contain ionophores

1 and **3**, respectively. Figure 4a shows the changes in electrical potential observed upon increasing the concentration of the creatininium cation (2-H^+) for the three different sensors in buffered water solution at pH 3.4. The blank sensor showed a very limited response at low concentrations of 2-H^+ ; however, at higher concentrations (above 10^{-4} M), the membrane displayed a Nernstian response ($59.2\text{ mV}/\log a_{\text{creatinine}}$). With the blank sensor, the partition equilibrium and subsequent changes in the electromotive force (EMF) signal are only driven by the lipophilicity of the creatininium ion, 2-H^+ . The effect of the addition of an ionophore in the membrane was shown for sensors **1** and **2**, for which a Nernstian response was observed at significantly lower concentrations of 2-H^+ . For sensor **2**, near ideal behavior was observed between $10\text{ }\mu\text{M}$ and 10 mM with a limit of detection (LOD) of $4.4 \pm 0.6\text{ }\mu\text{M}$. Interestingly, for sensor **1**, an ideal response was observed from $1\text{ }\mu\text{M}$ to 10 mM with a LOD one order of magnitude lower than for sensor **2**, $0.6 \pm 0.2\text{ }\mu\text{M}$. Taken together, these results suggest that the higher affinity displayed by ionophore **1** towards the creatininium cation, 2-H^+ , translated into a more sensitive ISE. Figure 4a shows the changes in EMF experienced by the three sensors when subjected to incremental changes in the creatininium concentration. Considering that the normal levels of creatinine range from 3 to 25 mM

in urine and from 0.06 to 0.42 mM in blood,^[25–27] both sensors **1** and **2** could be adequate for the analysis of real biological samples. However, the present challenge for the use of ISEs in real applications hinges on their selectivity, and not on their sensitivity.^[12]

Some of the most severe interferences observed when sensing large organic cations in biological samples arise from the presence of K^+ and Na^+ , which are typically vastly more prevalent than the creatininium cation.^[28,29] With this in mind, we performed selectivity studies to assess the interferences caused by these two inorganic cations (K^+ and Na^+) in the three prepared ISEs. Figure 4b depicts the EMF response of sensor **1** to increasing concentrations of creatinine, K^+ , and Na^+ . The selectivity coefficients of the three sensors for creatininium, potassium, and sodium cations were calculated from the corresponding calibration curves (Figure 5a,b). In Figure 5c, the obtained values are compared to the most stringent “required selectivity coefficients”, -1.9 orders of magnitude for K^+ and -3.4 orders of magnitude for Na^+ for creatinine sensing in the blood (see the Supporting Information for a detailed explanation on the required selectivity coefficients and the assumption on the error). Figure 5d depicts the same values expressed in units of concentration.

As seen in Figure 5a, the blank sensor showed a selectivity pattern paralleling the lipophilicity of the cations that was far from the required threshold of selectivity (Figure 5c). The introduction of ionophore **3** in the membrane (sensor **2**) improved the selectivity coefficients compared to the blank sensor (Figure S19). However, the selectivity values required for a useful ISE were only achieved with ionophore **1** (sensor **1**, Figure 5b). Sensor **1** displayed an enhanced potentiometric response for the creatininium cation compared to Na^+ and K^+ and afforded selectivity coefficients of -3.7 ± 0.1 and -2.5 ± 0.1 , respectively. Compared to the blank sensor, the selectivity of sensor **1** for 2-H^+ improved by more than one order of magnitude with respect to both interferences and exceeded the required threshold values by half an order of magnitude. All in all, the analytical parameters confirmed the superiority of sensor **1** and highlighted the importance of the enhanced interaction provided by the phosphonate group present in ionophore **1**. To evaluate whether these improvements could be transferred to practical applications, we studied the quantification of creatinine ions in real biological samples (urine and plasma) with sensor **1** (see the Supporting Information).

A key challenge for the application of ISEs in the analysis of biological fluids derives from biofouling, the unspecific response caused by the attachment of lipophilic components onto the surface of the polymeric membrane.^[30] We solved this issue of selectivity by taking advantage of the low limits of detection offered by this sensor and minimized the biofouling effect by sample dilution. Therefore, prior to analysis, urine and plasma samples were diluted by factors of 100 and 10, respectively. We selected samples from both healthy people and patients with renal dysfunction to assess the viability of the sensor for a broad range of creatinine concentrations.

After proper calibration of sensor **1**, diluted biological samples were analyzed. All of the measurements were compared to the standard reference method (the Jaffé

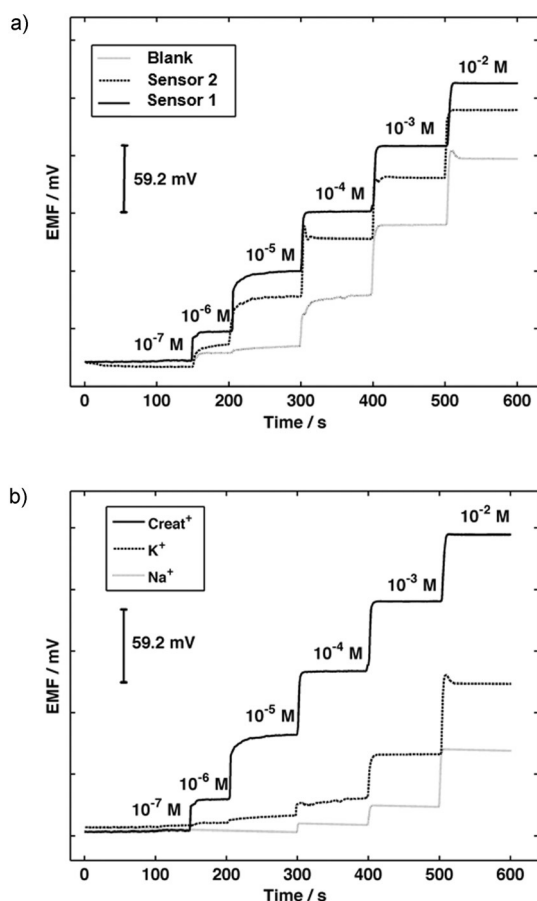


Figure 4. a) Response of the electromotive force (EMF) to incremental changes in the creatininium concentration (2-H^+). b) Response of the EMF of sensor **1** to incremental changes in the concentration of several cations.

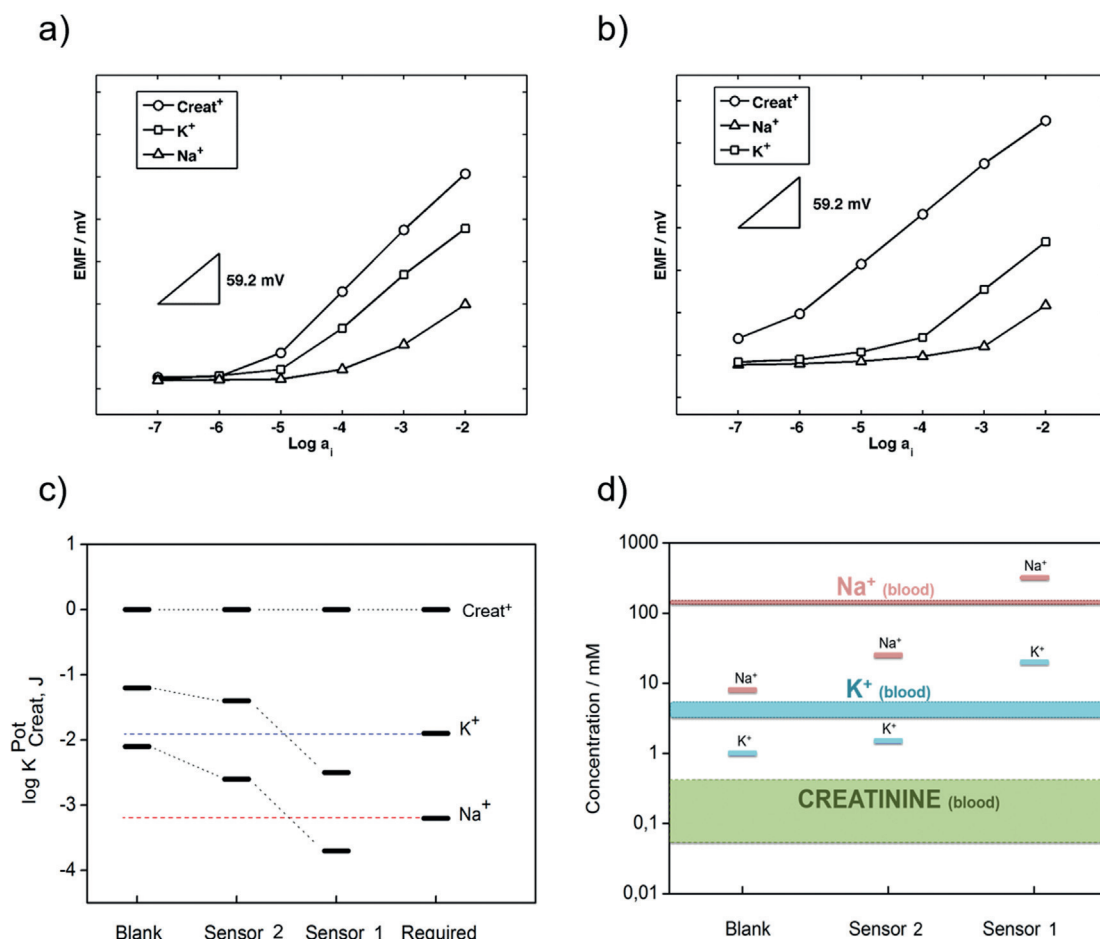


Figure 5. a, b) Calibration curves for 2-H^+ obtained with the blank sensor and sensor 1, respectively. c) Representation of the selectivity coefficients in logarithmic scale and d) threshold values in units of concentration, corresponding to the maximum allowed concentration of the interference ion at which the creatinine concentration can still be determined in real samples.

method)^[2] that is still routinely utilized in hospitals. The results obtained are shown in Figure 6; the values obtained with the Jaffé method were plotted versus those obtained with sensor 1. The data show an excellent linear correlation with a slope close to 1 and an intercept close to 0, demonstrating the validity of our method for the analysis of creatininum levels in real biological samples.

In conclusion, we have presented the first effective sensor for the selective potentiometric detection of the creatininum cation (2-H^+) in body fluids. The sensing membrane of the ISE incorporates the novel receptor **1**, which is capable of establishing a three-dimensional array of intermolecular interactions with 2-H^+ , which is included in its deep and polar aromatic cavity. The binding manifold responsible for the excellent selectivity of receptor **1** towards 2-H^+ has been studied and analyzed in detail. The application of receptor **1** in an ISE unveiled a potentiometric sensor with outstanding performance in terms of sensitivity and selectivity. This sensor readily detected and quantified the amount of creatininum cation, 2-H^+ , in both urine and plasma. We hope that the described sensor device 1 will have a significant impact on current and future healthcare development.

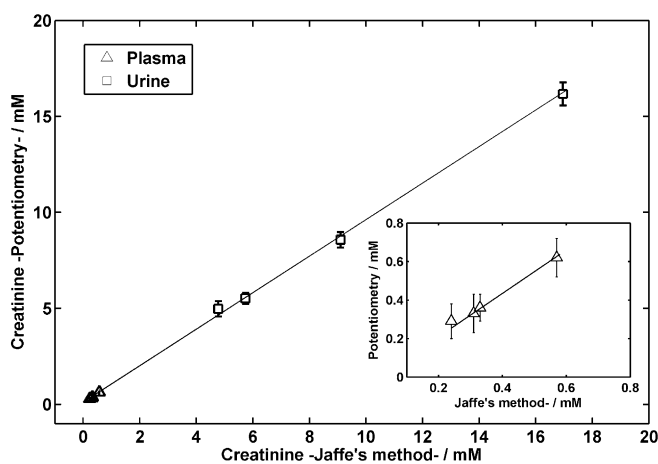


Figure 6. Linear correlation of the creatinine concentrations determined by potentiometric (ordinate) and colorimetric (abscissa) methods for different plasma and urine samples. The inset shows the linear regression for plasma samples only.

Acknowledgements

We thank Gobierno de España MINECO (CTQ2014-56295-R, CTQ2014-52974-REDC, CTQ2013-46404-R, and Severo Ochoa Excellence Accreditation 2014-2018 SEV-2013-0319), FEDER funds (CTQ2014-56295-R), the Ramón y Cajal Programme, FPI fellowship (BES-2011-048297), and the ICIQ Foundation for funding. We would also like to acknowledge financial support from the European Union, a Marie Curie Grant (PCIG09-GA-2011-293538; Project FlexSens), and the Fundación Recercaixa (Project SensAge). We thank Eduardo C. Escudero-Adán for help with the analysis of the X-ray crystallographic data.

Keywords: cavitands · creatinine · ionophores · molecular recognition · sensors

How to cite: *Angew. Chem. Int. Ed.* **2016**, *55*, 2435–2440
Angew. Chem. **2016**, *128*, 2481–2486

- [1] J. R. Delanghe, M. M. Speeckaert, *NDT plus* **2011**, *4*, 83–86.
- [2] J. M. Pizzolante, United States, US4818703 A, **1989**.
- [3] R. M. Jacobs, J. H. Lumsden, J. A. Taylor, E. Grift, *Can. J. Vet. Res.* **1991**, *55*, 150–154.
- [4] D. Stockl, H. Reinauer, *Clin. Chem.* **1993**, *39*, 993–1000.
- [5] L. M. Thienpont, A. P. Deleenheer, D. Stockl, H. Reinauer, *Clin. Chem.* **1993**, *39*, 1001–1006.
- [6] T. W. Bell, N. M. Hext, A. B. Khasanov, *Pure Appl. Chem.* **1998**, *70*, 2371–2377.
- [7] T. Bell, A. Firestone, J. Liu, R. Ludwig, S. Rothenberger in *Inclusion Phenomena and Molecular Recognition* (Ed.: J. Atwood), Springer, New York, **1990**, pp. 49–56.
- [8] T. W. Bell, Z. Hou, Y. Luo, M. G. B. Drew, E. Chapoteau, B. P. Czech, A. Kumar, *Science* **1995**, *269*, 671–674.
- [9] D. L. Beckles, J. Maioriello, V. J. Santora, T. W. Bell, E. Chapoteau, B. P. Czech, A. Kumar, *Tetrahedron* **1995**, *51*, 363–376.
- [10] P. Bühlmann, W. Simon, *Tetrahedron* **1993**, *49*, 7627–7636.
- [11] P. Bühlmann, M. Badertscher, W. Simon, *Tetrahedron* **1993**, *49*, 595–598.
- [12] P. Bühlmann, E. Pretsch, E. Bakker, *Chem. Rev.* **1998**, *98*, 1593–1687.
- [13] P. Bühlmann, L. D. Chen in *Supramolecular Chemistry: From Molecules to Nanomaterials* (Eds.: P. A. Gale, J. W. Steed), Wiley, Hoboken, **2012**, pp. 2539–2579.
- [14] P. M. Kelly, R. Katak, D. Parker, A. F. Patti, *J. Chem. Soc. Perkin Trans. 2* **1995**, 1955–1963.
- [15] P. Bühlmann, P. G. Boswell, PCT/US06/20366, United States, **2008**.
- [16] B. Verdejo, G. Gil-Ramirez, P. Ballester, *J. Am. Chem. Soc.* **2009**, *131*, 3178–3179.
- [17] D. Hernández-Alonso, S. Zankowski, L. Adriaenssens, P. Ballester, *Org. Biomol. Chem.* **2015**, *13*, 1022–1029.
- [18] M. Ciardi, A. Galán, P. Ballester, *J. Am. Chem. Soc.* **2015**, *137*, 2047–2055.
- [19] M. Ciardi, F. Tancini, G. Gil-Ramirez, E. C. Escudero Adán, C. Massera, E. Dalcanales, P. Ballester, *J. Am. Chem. Soc.* **2012**, *134*, 13121–13132.
- [20] P. Anzenbacher, K. Jursikova, V. M. Lynch, P. A. Gale, J. L. Sessler, *J. Am. Chem. Soc.* **1999**, *121*, 11020–11021.
- [21] L. Bonomo, E. Solari, G. Toraman, R. Scopelliti, M. Latronico, C. Floriani, *Chem. Commun.* **1999**, 2413–2414.
- [22] CCDC 1431012 (**2c1**) and 1431013 (BARF[−]·2H⁺) contain the supplementary crystallographic data for this paper. These data can be obtained free of charge from The Cambridge Crystallographic Data Centre.
- [23] S. K. Kim, J. L. Sessler, *Acc. Chem. Res.* **2014**, *47*, 2525–2536.
- [24] J. Gao, Y. Hu, S. Li, Y. Zhang, X. Chen, *Chem. Phys.* **2013**, *410*, 81–89.
- [25] M. W. Taal, G. M. Chertow, P. A. Marsden, K. Skorecki, A. S. L. Yu, B. M. Brenner, *Brenner & Rector's The Kidney*, 9th ed., Elsevier Saunders, Philadelphia, **2012**.
- [26] E. Davila, L. B. Gardner, *Cancer* **1987**, *60*, 161–164.
- [27] G. Ohara, K. Miyazaki, K. Kurishima, K. Kagohashi, H. Ishikawa, H. Satoh, N. Hizawa, *Oncol. Lett.* **2012**, *3*, 303–306.
- [28] K. Ueda, R. Yonemoto, K. Komagoe, K. Masuda, N. Hanioka, S. Narimatsu, T. Katsu, *Anal. Chim. Acta* **2006**, *565*, 36–41.
- [29] J. Ampurdanés, G. A. Crespo, A. Maroto, M. A. Sarmentero, P. Ballester, F. X. Rius, *Biosens. Bioelectron.* **2009**, *25*, 344–349.
- [30] P. Bühlmann, M. Hayakawa, T. Ohshiro, S. Amemiya, Y. Umezawa, *Anal. Chem.* **2001**, *73*, 3199–3205.

Received: October 30, 2015

Revised: December 10, 2015

Published online: January 8, 2016